

Buffer-free Class-Incremental Learning with Out-of-Distribution Detection

Srishti Gupta^{a,b}, Daniele Angioni^a, Maura Pintor^a, Ambra Demontis^a, Lea Schönherr^d, Battista Biggio^a, Fabio Roli^{a,c}

^aDIEE, University of Cagliari, Via Marengo 2, Cagliari, 09100, Italy

^bDIAG, Sapienza University of Rome, Via Ariosto 25, Rome, 00185, Italy

^cDIBRIS, University of Genova, Via Dodecaneso 35, Genova, 16146, Italy

^dCISPA Helmholtz Center for Information Security, Stuhlsatzenhaus 5, Saarbrücken, 66123, Germany

Abstract

Class-incremental learning (CIL) poses significant challenges in open-world scenarios, where models must not only learn new classes over time without forgetting previous ones but also handle inputs from unknown classes that a closed-set model would misclassify. Recent works address both issues by (i) training multi-head models using the *task-incremental learning* framework, and (ii) predicting the task identity employing *out-of-distribution* (OOD) detectors. While effective, the latter mainly relies on joint training with a memory buffer of past data, raising concerns around privacy, scalability, and increased training time. In this paper, we present an in-depth analysis of post-hoc OOD detection methods and investigate their potential to eliminate the need for a memory buffer. We uncover that these methods, when applied appropriately at inference time, can serve as a strong substitute for buffer-based OOD detection. We show that this buffer-free approach achieves comparable or superior performance to buffer-based methods both in terms of class-incremental learning and the rejection of unknown samples. Experimental results on CIFAR-10, CIFAR-100 and Tiny ImageNet datasets support our findings, offering new insights into the design of efficient and privacy-preserving CIL systems for open-world settings.

Keywords: continual learning, out-of-distribution detection, neural networks.

1. Introduction

Rapid advancements in machine learning (ML) have enabled remarkable successes across multiple applications, such as computer vision [1] and natural language processing [2]. However, when deployed in the open world, such models have to face two major issues. First, traditional ML models are designed in a *closed-set* perspective, which expects all data to be Independent and Identically Distributed (i.i.d.), i.e., to come from one of the distributions seen during training. This is in contrast to the *open-set* nature that characterizes the real world, where the model will inevitably receive and misclassify inputs from unknown classes or distributions as belonging to one of the learned ones, generating classification errors for inputs that should instead be rejected [3, 4]. Second, the model must be frequently updated to include new classes, quickly becoming infeasible when considering the significant financial costs of a single training session, computational resources, and environmental impacts [5].

The field of *out-of-distribution* (OOD) detection develops methods for recognizing and rejecting inputs from unknown classes (or unknown distributions) at inference time [6, 7]. Conversely, *incremental learning* (IL) field focuses on continually updating models with new knowledge assuming the unavailability of old data without losing old representations. While the two parallel lines of research have evolved to mitigate these

problems separately, there is only limited work targeting the issue jointly.

In principle, IL algorithms are required to gradually acquire new knowledge with little to no access to past data [8], so that the storage and computational complexity do not increase over time. Such requirements can cause the model to experience the phenomenon of *catastrophic forgetting*, wherein the model drastically forgets previously-learned knowledge [9], as gradient-based optimization potentially overwrites important parameters relevant to earlier data in favor of the newly acquired ones. One prominent IL scenario is *task-incremental learning* (TIL), where each task typically corresponds to a disjoint set of classes [10]. Most recent TIL approaches employ multi-head models [11], i.e., a model architecture comprising (i) a shared backbone and (ii) different task-specific classifiers mounted on top, also referred to as *heads*. Here, the shared backbone and current head are updated with ad-hoc strategies that allow near-perfect elimination of catastrophic forgetting [11]. During inference, the task identity (task-id) is provided, directing the input sample to its head of specialization. For instance, consider a model required to learn two tasks sequentially, comprised of two classes each: $t_0 \in \{cat, dog\}$, and $t_1 \in \{duck, frog\}$. During inference, a sample is passed through the shared backbone and a classifier is assigned based on the given task-id, e.g., if the sample belongs to t_1 , the sample is forwarded to the second head, and classification is performed only between classes: “duck” and “frog”.

Despite the efficacy of multi-head models, assuming task-

Email addresses: srishti.gupta@uniroma1.it (Srishti Gupta), ambra.demontis@unica.it (Ambra Demontis)

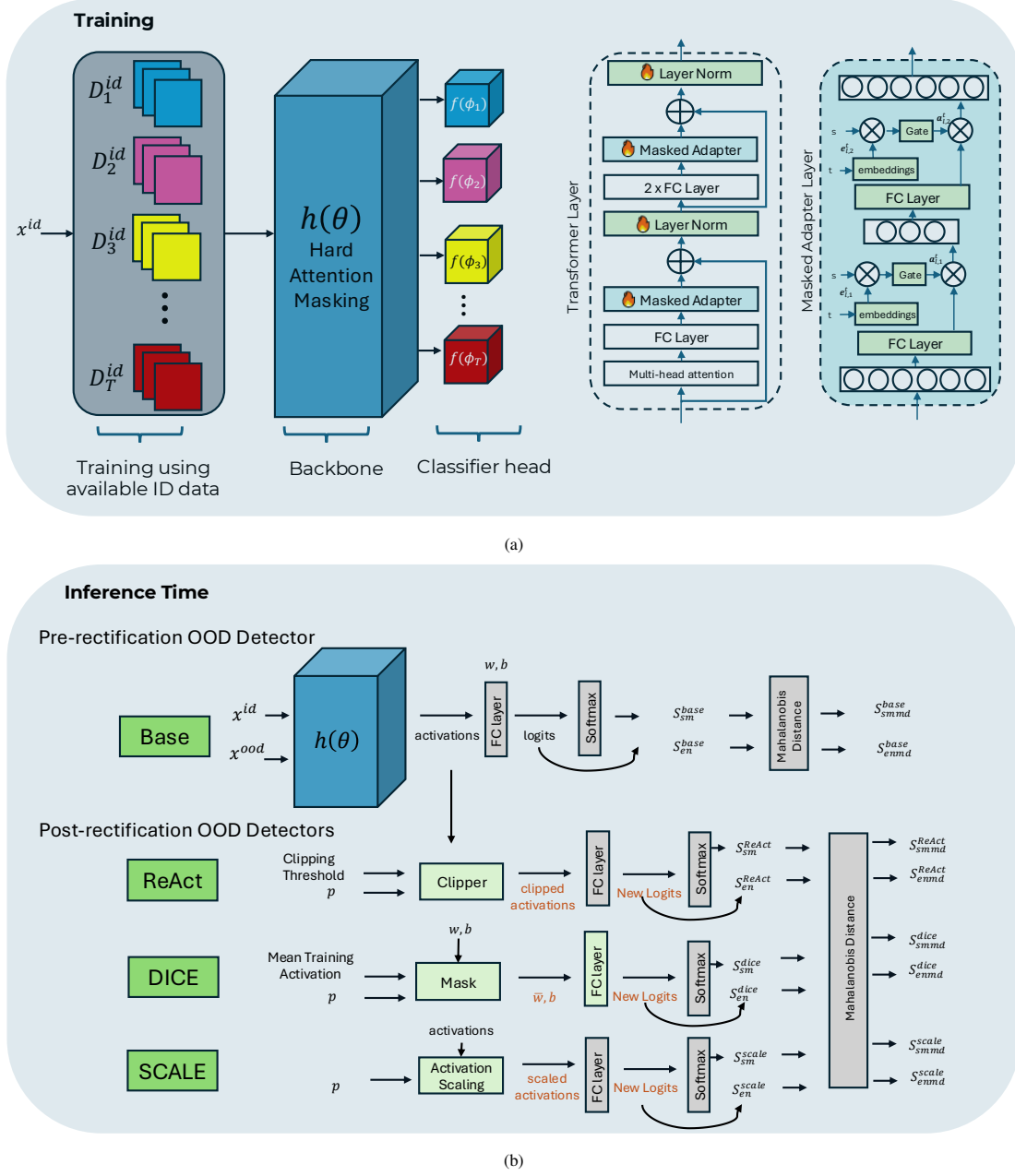


Figure 1: Graphical representation of a) training a buffer-free multi-head system with dedicated head for individual task, using masked adapter layer in its transformer layers, b) inference time functionality of OOD detectors per head, operating in the output space, to increase the separability of IND from OOD samples.

id availability at test time is highly unrealistic [12]. Therefore, a more practical yet challenging scenario, known as *class-incremental learning* (CIL), requires the models to classify input samples across all previously learned classes without task information [13]. Recent theoretical and empirical studies [14] demonstrated that solving a CIL problem requires solving two problems simultaneously: (i) *task-id prediction* (TP), i.e., predicting the correct task-id, and (ii) *within-task prediction* (WP), i.e., predicting the correct class when the task-id is given. Given that TIL models already excel in WP performance, recent works addressed the missing step, i.e., strong TP, by integrating OOD detection techniques [15–17]. In particular, they make use of a

memory buffer composed of samples from past tasks and train each head to detect OOD samples from different tasks, thus, using this mechanism to perform task-id prediction. Moreover, some works have also shown that, in addition to predicting task-id, this type of model can also recognize never-before-seen samples at inference, making them the ultimate choice for reliable and efficient deployment in an open-world setting [15]. However, relying on memory buffers introduces significant limitations. Privacy concerns arise as the storage of data from past tasks may violate regulations such as GDPR¹, especially in

¹General Data Protection Regulation <https://gdpr-info.eu>

sensitive applications like healthcare and finance. Employing a buffer facilitates data breaches and, as only a few examples for each class are retained by it and employed to train the model avoiding forgetting, they will have a high influence on the decision of the classifier, which facilitates ML poisoning [18] and privacy attacks [19]. Additionally, replay buffers introduce scalability issues, as increasing the number of tasks significantly amplifies memory and computational requirements, making these models difficult to deploy in resource-constrained environments [20].

In this work, we argue that a memory buffer is not necessary for a strong task-id prediction. Instead, we show that it is sufficient to employ appropriate *post-hoc OOD detection* techniques, i.e., methods that detect unknown inputs at inference time without requiring additional training or architectural changes [6, 7, 21–24]. They are also capable of detecting unseen OOD samples at inference. Comprehensive experimental evaluations of different kinds of post-hoc detection methods conducted on CIFAR-10, CIFAR-100 and Tiny ImageNet datasets validate our findings, revealing that this approach not only retains competitive CIL performance compared to methods relying on memory buffers but also outperforms them in open-set recognition capabilities.

To summarize, the main contributions of this work are the following:

- We perform an in-depth analysis to assess the effectiveness of a state-of-the-art buffer-based CIL method named MORE when combined with different OOD detectors and scoring functions;
- We propose BUILD, which obtains performances comparable to MORE without using a buffer. We also observed that while BUILD is comparable to MORE, it is also more stable across all scoring methods;
- We show threshold-free rejection performance on varying rejection rates to properly evaluate the open-world performance.

Thus, we believe that our analysis unveils a lightweight and secure alternative to incremental training in an open-world setting that is otherwise popularly dominated by buffer-based methods.

In the following, we first present a formalization of the incremental learning problem and the main methods to prevent forgetting (Sect. 2), then present our proposed method (Sect. 3). Then, we present the experimental protocol and discuss the results to validate our method (Sect. 4), we discuss the related work (Sect. 5 and our conclusions (Sect. 6).

2. Background

In this section, we introduce the main problem formulation of incremental learning and its open problems (Sect. 2.1). To complete the overview of current techniques, we present the main competitor of our method, which uses a combination of

multi-head models, OOD detectors, and memory buffers to implement a CIL scenario while also trying to solve the open problems mentioned below (Sect. 2.1.1). We conclude this section by presenting existing algorithms for post-hoc OOD detection (Sect. 2.2).

2.1. Class-Incremental Learning (CIL)

Let us consider a *class-incremental learning* (CIL) scenario, where the set of classes $y \in \mathcal{Y}$ must be learned incrementally. Here, an ML model is required to learn them as a sequence of tasks $t = 1, 2, \dots, T$. Each task is characterized by its input space \mathcal{X}^t , label space $\mathcal{Y}^t \subseteq \mathcal{Y}$, and dataset $D^t = \{(\mathbf{x}_i^t, y_i^t)\}_{i=1}^{n_t}$ with n_t training instances, where $\mathbf{x}_i^t \in \mathcal{X}^t$ and $y_i^t \in \mathcal{Y}^t$, such that there is not class overlapping between different tasks (i.e., $\mathcal{Y}_t \cap \mathcal{Y}_{t'} = \emptyset$ for $t \neq t'$). We denote $\mathcal{Y}^{\leq t} = \cup_{k=1}^t \mathcal{Y}^k$ as the cumulative label space composed of all classes from task 0 to task t . Accordingly, a universal label space \mathcal{Y} can be defined as $\mathcal{Y}^{\leq T}$ where T is the oracle class, set of all possible classes. When learning a new task t , the CIL model f_t is required to learn the optimal function $f^t : \mathcal{X}^{\leq t} \rightarrow \mathcal{Y}^{\leq t}$ that maps an input sample to its correct label from either the current task t or the previous.

Kim et al. [14] demonstrated that, given an input sample \mathbf{x} , the output probability of a CIL model can be decomposed into two probabilities, known as (i) *within-task prediction* (WP) and (ii) *task-id prediction* (TP):

$$P(y_j^t | \mathbf{x}) = \underbrace{P(y_j^t | \mathbf{x}, t)}_{\text{WP}} \cdot \underbrace{P(t | \mathbf{x})}_{\text{TP}} \quad (1)$$

where TP is the probability that \mathbf{x} belongs to one of the classes from task t , where TP is the probability that \mathbf{x} belongs to one of the tasks the model was incrementally trained upon. and WP is the probability that the correct class label is j given the task-id t .²

Forgetting past knowledge. Catastrophic forgetting represents an open challenge for IL. While updating the model to learn new tasks requires changing its parameters, this causes the trained model to abruptly lose previously acquired knowledge. This phenomenon is particularly pronounced in training processes that lack explicit mechanisms for knowledge retention, as these methods tend to update parameters globally without consideration for preserving previously-learned tasks [25]. The most popular IL methods rely on *replay* (or *rehearsal*). The idea is to store samples from old tasks in a memory buffer that can be replayed alongside the current task when learning it.

Open-world conditions. The open-world condition represents a particularly demanding scenario in IL, as models must not only avoid catastrophic forgetting but also effectively identify and handle novel OOD samples. When operating in unconstrained environments, these systems inevitably encounter samples that fall outside the distributions of previously learned tasks. Standard models, without explicit novelty detection mechanisms, tend to force-fit these unknown samples into their existing learned

²In the TIL setting, the first term is replaced by knowing exactly the task-id information, which is passed together with the input sample during inference.

tasks, producing fundamentally incorrect predictions. We want to make an important distinction here that OOD detection with respect to a task is useful to predict task-id (or perform TP), whereas, when detecting OOD with respect to the system itself, we refer to the conventional setting of detecting never-before-seen (*wild*) samples.

2.1.1. MORE

A recent approach called Multi-head model for continual learning via OOD REplay (MORE) [15] tried to solve the aforementioned gaps. MORE combines (i) a multi-head transformer architecture to learn tasks incrementally, (ii) masked adapter modules in the transformer layers to isolate the learning and mitigate forgetting, and (iii) OOD detectors and replay buffers to perform task-id prediction. This is an important step towards non-forgetting CIL models in open-world conditions. First, the use of a multi-head architecture creates separate classifiers (heads) for each task, mitigating forgetting by letting the previous heads mostly unchanged. To achieve this, MORE uses OOD detection to enable distinction between tasks without explicit boundaries (i.e., to adapt the multi-head architecture to the CIL setting). They used Mahalanobis Distance as a coefficient to softmax scores as OOD scores. Additionally, MORE combines OOD detection with the use of a buffer to store exemplar samples from previous tasks. Specifically, it uses the saved samples to provide the classification heads with OOD capabilities for task-id prediction in CIL setting.

Multi-head Transformer Models for Incremental Learning. Architecturally, a general multi-head setup for incremental learning is composed of (i) a fixed pre-trained backbone h with parameters θ , (ii) a set of task-specific trainable adapters with parameters ϕ_t inserted in each transformer layer [26], and (iii) a set of classification heads f_t on top of the backbone, with parameters w_t for a given task t . We now define as h_t the backbone that extracts the features using the adapter ϕ_t specialized on task t . In the following, if not specified, we refer to as $f_t(\mathbf{x})$ the output of the overall model $f_t(h_t(\mathbf{x}))$ when task t is selected. Training the model on the task t amounts to finding the optimal configuration of ϕ_t and w_t that minimize the classification loss, e.g., the cross-entropy.

In MORE, the multi-head architecture is trained with a 2-step process. In the first step, f_t is trained on the dataset D_t and M , where the latter is a memory buffer containing samples from previous tasks. The memory buffer is the leading responsible to achieve TP, and is used to train an additional logit on f_t to recognize as OOD samples from different tasks. The objective can then be defined as follows:

$$\arg \min_{f_t} \sum_{(\mathbf{x}, y) \sim D_t} \mathcal{L}(f_t(\mathbf{x}), y) + \sum_{(\mathbf{x}, y) \sim M} \mathcal{L}(f_t(\mathbf{x}), OOD) \quad (2)$$

We refer to MORE-FW the model resulting from this optimization process.

In a second step, referred to as *back-update*, all previous heads are updated to recognize as OOD also samples from the relatively future tasks, e.g., f_1 is updated with samples from

tasks $2, \dots, t$. This result in the following optimization process:

$$\arg \min_{w_j} \sum_{(\mathbf{x}, y) \sim \tilde{D}_j} \mathcal{L}(f_j(\mathbf{x}), y) + \sum_{(\mathbf{x}, y) \sim M} \mathcal{L}(f_j(\mathbf{x}), OOD) \quad (3)$$

where \tilde{D}_j contains the data from task j sampled from M , and \tilde{M} contains randomly selected samples from D_t and the remaining OOD samples from M (OOD w.r.t. task j). We note that in this step only the parameters of the previous heads are finetuned. We refer to this last version as MORE, and consider both MORE-FW and MORE for the analysis in Sect. 4.

Minimizing Forgetting with Parameter Isolation. To prevent interference among parameters, HAT isolates subsets of the model parameters for each task [27–29].

For a layer l , and a task $t + 1$, the embedding e_l^t will protect the neurons essential for the previous task and should output a value equal to 0 for the neurons important for the task t and 1 for the neurons not important for that task. Since the step function is not differentiable, a sigmoid function can approximate it, obtaining the attention mask $a_l^t = \sigma(se_l^t)$. This mask will then be multiplied by the output of layer l during training so that the neurons for the task t are not updated. This mechanism preserves the attention values for units that were important for previous tasks while leaving the other neurons to condition on future tasks (see masked adapter block in Fig. 1).

OOD Replay Mechanism. At test time, the model can be subjected to either IND or OOD classes: $\mathbf{x} \in \{\mathbf{x}_{ind}, \mathbf{x}_{ood}\}$ such that $\mathbf{x}_{ood} \in \mathcal{D}_k^{ood}$ where $k \neq t$, as expected in the wild. OOD detection methods, borrowed from the OOD literature, are used for TP. MORE uses the replay mechanism of saved samples from past tasks to build new classification heads without altering previously learned knowledge.

Limitations of MORE. The main limitations of MORE are related to its usage of a memory buffer. They use the memory buffer to expose outliers to individual heads, which is less attractive in real-world setting. While using memory buffers has shown a great boost in performance, they have major drawbacks: a) Limited scalability: as the number of classes grow, these methods require additional computation and storage of raw input samples. Even if the memory size is fixed, the ability of the sample sets to represent the original distribution deteriorates; b) Privacy issues: storing data is not always a compliant option, especially for finance and healthcare data. Storing data leaves larger surface area for attacks [30] against ML systems; c) Task-recency bias: typically a dominant task bias is observed towards the more recent classes, which may be caused due to imbalance in current and past samples; d) Memory storage: storing raw samples to buffer consumes enormous memory costs making the process computationally expensive.

2.2. Post-hoc OOD Detectors

Given a well-trained model, post-hoc OOD detectors modify the intermediate results to enhance the separability of IND and OOD samples. They have a low computational cost and require minimal modifications in a plug-and-play manner to the models [31]. In this work, we consider the following state-of-the-art post-hoc OOD detection methods in a multi-head setup:

ReAct [22], which thresholds the activation value of the penultimate layer of neural networks at test time; *DICE* [23], which ranks, at test time, the importance of the units to the classification, averaged over classes, and considers only the most important units; and *SCALE* [24], which scales all the activations equally by a factor r and then thresholds them to identify OOD samples. The scaling factor r is computed as the ratio of the sum of all the activations versus the sum of the activations with a value higher than the p^{th} percentile of the activations.

We also consider other OOD detectors, using them as scoring functions \mathcal{S} , as in [22–24]. In particular, we consider the following scoring functions: *Max Softmax Probability (MSP)* [6], which thresholds the softmax outputs to predict the sample as IND or OOD; and *Mahalanobis Distance (MD)* [21], which assumes that the pre-trained features can be fitted well by a class-conditional Gaussian distribution. They define C class-conditional Gaussian distributions $\mathcal{N}(f(\mathbf{x})|\mu_c, \Sigma)$, where μ_c is the mean for class $c \in \{1, \dots, C\}$ and Σ the covariance matrix, which are estimated on the training samples to obtain $\hat{\mu}_c$ ($\hat{\Sigma}$). Then, they define the confidence score $M(\mathbf{x})$ as the Mahalanobis distance between the test sample \mathbf{x} and the closest class-conditional distribution: $M(\mathbf{x}) = \max_c -(f(\mathbf{x}) - \hat{\mu}_c)^T \hat{\Sigma}^{-1} (f(\mathbf{x}) - \hat{\mu}_c)$. We also consider *Energy (EN) Score* [7], which applies an energy function to a discriminative model, with energy defined as $E(\mathbf{x}; f) = -v \log \sum_i^K e^{f_i(\mathbf{x}/v)}$, being v the temperature parameter. High energy can be interpreted as a low likelihood of occurrence.

3. Post-hoc OOD Detection for CIL

We now present our novel framework, named BUILD. By removing the buffer, we entirely use post-hoc detectors to perform task-id prediction, without changing the TIL training process which already have great results.

3.1. Pipeline

A high-level overview of BUILD can be seen in Fig. 1, where the upper box refers to the training time and the lower box to the inference time. BUILD inherits the same structure of MORE models as described in Sect. 2.1.1.

Training. To train the task classifier t , the training set \mathcal{D}_{ind}^t with c in-distribution classes: $\forall (\mathbf{x}, y) \in \mathcal{D}_{ind}^t$ and $\{y_1, y_2, \dots, y_c\} \in \mathcal{Y}_{ind}^t$ is used to update the parameters ϕ^t and \mathbf{w}^t while leaving the original backbone parameters θ and the parameters of previously trained task classifiers $\phi^{\leq t}$, $\mathbf{w}^{\leq t}$ unchanged (thanks to masked adapters). We also note that BUILD does not expose outliers during training as done in previous work [15, 16], nor does it use time-consuming solutions such as back-update on the classification heads. In practice, each classifier head is exclusively trained on the corresponding task-specific dataset (see training in Fig. 1) solely optimizing the left-hand term Eq. 2.

Inference. At test time, after training task t , the model can be subjected to either IND or OOD classes: $\mathbf{x} \in \{\mathbf{x}_{id}, \mathbf{x}_{ood}\}$ such that $\mathbf{x}_{ood} \in \mathcal{D}_{ood}^{t'}$ where $t' \neq t$, as expected in the wild. When the system operates in a close-world setting: $\mathbf{x} \in \mathcal{D}^{\leq t}$, task-id prediction is performed. This is done by maximizing the

OOD scores derived from each head to assign the task-id, consequently the class. However, when the system is deployed in open-world setting, OOD scores are evaluated based on their probability of being rejected as OOD.

3.2. Combining OOD Detectors and Scoring Functions

The OOD scores are the output scores that are used to evaluate the OOD-ness of the sample. Based on the OOD detector, the OOD scores can be derived at any output stage: activations, logits, or probability space. Following our framework, we can choose Γ as an post-hoc OOD detector, such as ReAct, DICE or SCALE. In this case, Γ wraps the last part of the network starting from the penultimate layer of the task classifier t to extract activations $\mathbf{z}_t = h_t(\mathbf{x})$ as shown in the inference block in the Fig. 1. The OOD detector Γ is then used to obtain the new activations $\bar{\mathbf{z}}_t = \Gamma(\mathbf{z}_t)$. The modified features are then used to perform OOD detection:

$$f_t^\Gamma(\mathbf{x}, \theta) = \mathbf{w}_t \times \bar{\mathbf{z}}_t + b_t \quad (4)$$

Since DICE performs modification in the weights of the last fully-connected layer instead of the output space, we can rewrite Eq. 4 for DICE as:

$$f_t^\Gamma(\mathbf{x}, \theta) = M * \mathbf{w}_t \times \mathbf{z}_t + b_t \quad (5)$$

where M are the masks for important units from the classification layer. Depending on the scoring function \mathcal{S} , the final scores can be represented as $\mathcal{S}(f_t^\Gamma(\mathbf{x}, \theta))$. In this work, we analyze the performance of the OOD detectors across four scorers a.k.a. \mathcal{S} (mentioned in Sect. 2): (i) Softmax (SM) scores: Applying softmax at the final layer and getting the maximum for final output, basically MSP; (ii) MD as coefficient to SM (SMMD) scores (as in [15]); (iii) Energy (EN) scores, mapping the logit outputs from the network $f(\mathbf{x})$ to a scalar value; and (iv) MD applied to EN (ENMD) scores, using the same mean and covariance parameters from the training data.

After we get these scores, we can evaluate the model for closed-world and open-world settings. For a given detector Γ , we can also compute task-id :

$$\hat{y}^\Gamma = \arg \max_{1 \leq t \leq T} \bigoplus_{1 \leq t \leq T} \mathcal{S}(f_t^\Gamma(\mathbf{x}, \theta)) \quad (6)$$

where \bigoplus is the concatenation over the output space.

4. Experiments

In this section, we first define the experimental setup and then discuss the results obtained by comparing the baseline method with the buffer-free method: BUILD. We also analyze the results by considering all the configurations of the scoring function and OOD detectors for these models and discuss the best practices.

4.1. Experimental Setup

Baseline. We consider MORE as our baseline. In our experiments, we leveraged the implementation provided by its authors. We analyze not only the version proposed by the authors but also the intermediate variant MORE-FW, and then the method BUILD under different OOD methods, including pre- and post-rectification and scoring functions. We finally do an ablation study, where we consider the best-performing post-hoc OOD detector for each method.

Backbone. We use the following architecture: DeiT-S/16 [32] with 2-layer adapter module [26] with 64-dimensional latent space in each transformer layer. We borrowed the checkpoints of the backbone transformer from the baseline work where Vision Transformer (ViT) is pre-trained on ImageNet classes after removing 389 classes that are similar to the classes in CIFAR datasets to avoid data leaking at train time [15]. We plug OOD detectors into the output space.

Evaluation Metrics. We group the evaluation metrics into Closed- and Open-world performance metrics.

Closed-world Performance. The metrics here are defined to evaluate the model’s performance on seen classes and how well the model can predict the correct class in the incremental learning setup.

- Last Classification Accuracy (LCA). Accuracy of all seen classes after the last task T is trained: $LCA = A^T$.
- Average Incremental Accuracy (AIA). Average of all the accuracies computed after each incremental step: $AIA = 1/T \sum_{t=1}^T A^t$.
- Average Forgetting (AF): Forgetting refers to the performance decline of the task classifier after training task t when compared to the performance when the task head was first learned. The reported results are averaged considering all seen tasks. $\mathcal{F} = 1/(T-1) \sum_{t=1}^{T-1} \{A_t^{init} - A_t^T\}$.

Open-world Performance. The metrics used here are used to assess the performance of the models on unseen classes and how distinguishable the scores of seen vs unseen samples are for different detectors. We also note that comparing detectors is not as straightforward as evaluating accuracy. For detection, we consider two classes: positive (IND) and negative (OOD). An important consideration is the shift in the ratio of IND to OOD data after each incremental training. For e.g., in CIFAR10-5T, after the first training, IND is 20% of the test data, while OOD is 80%, which changes by the time we have trained the second last task to: IND to 80% and OOD to 20%. Therefore, we calculate the metrics after each training until the second-to-last model and average it.

- Average Area Under the Curve (AUC). AUC [33] is a threshold-independent metric that computes the area under the ROC curve, i.e., how TPR varies against an increasing FPR. During incremental training, the ratio of the two classes continuously changes; thus, we calculate the AUC after each incremental step and average it.

- Average Area Under Precision-Recall (AUPR). As mentioned in [34], AUPR is a suitable metric for imbalanced datasets where positive and negative classes can have differing base rates. We average the AUPR as we do for the AUC.

Datasets. We run our experiments on three image classification datasets: CIFAR10, CIFAR100, and TinyImageNet200. CIFAR10 is composed of 60,000 32×32 RGB images of 10 classes. Per class, there are 5000 samples for training and 1000 samples for testing. We consider CIFAR10-5T where a sequence of 5 tasks, composed of 2 classes each, is trained, without changing the original class order, e.g., task t_0 comprises samples from class 0, 1; task t_1 samples from class 2, 3, etc. CIFAR100 is composed of 60,000 32×32 RGB images of 100 classes with 500 samples for training and 100 samples for testing in each class. We conduct experiments for two settings: (i) CIFAR100-10T: sequence of 10 tasks: t_0, \dots, t_9 , each task composed of 10 classes, is used to train the model; and (ii) CIFAR100-20T: sequence of 20 tasks: t_0, \dots, t_{19} , each task composed of 5 classes is used to train the model. TinyImageNet200 is composed of 120,000 64×64 color images of 200 classes with 500 samples for training, 50 for validation and 50 for testing in each class. Following previous works [15], we use validation dataset for testing since test set doesn’t have labels.

Training Details. We train the task-specific adapters, normalization layers, and classification heads using the stochastic gradient descent (SGD) optimizer for N epochs with learning rate α , and batch size s .

CIFAR10-5T: We set $N = 20$, $\alpha = 0.005$ and $s = 64$ for both settings. The bottleneck size of the adapter is 64. Additionally, for MORE, we set a buffer size of 200 and an additional 10 epochs for the back-update procedure.

CIFAR100-20T: We set $N = 40$, $\alpha = 0.005$ and $s = 64$ for both settings. The bottleneck size of the adapter is 64. For MORE, we use the default setting with a buffer size of 2000 and an additional 10 epochs for back-update.

CIFAR100-10T: We used the same hyperparameters as CIFAR100-20T except for $\alpha = 0.001$, as we have more classes in each training round.

T-Imgnet200-5T: We used $N=25$, $\alpha=0.005$, $s=64$. The bottleneck size is 128. For MORE experiments the buffer size is 2000 samples in the memory. As in the original work, they do not perform backupdate for this dataset, therefore, we only perform forward pass and consequently refer to them as MORE-FW.

T-Imgnet200-10T: We used similar settings as T-Imgnet200-5T except for $N=20$.

For OOD detection at inference, we save certain parameters at the train time that are used later e.g., the mean and standard deviation of each class and task to compute Mahalanobis Distance, mean activations, and clipping threshold employed by DICE and ReAct, respectively. SCALE does not require any parameters from train time. For rectification, we use the percentile value p recommended in the respective original paper i.e., 90, 85, 85 for ReAct, DICE, and SCALE, respectively.

Task-id Prediction. At inference time, we first compute task-

id prediction using OOD detectors. As shown in Fig. 1, OOD detectors are deployed at different stages of the output space depending on the detector type. We first compute the detection method from the baseline method (Base) acting before the rectification, i.e., Softmax scores with and without the combination with Mahalanobis Distance (MD), referred to as SM and SMMD. At this *Base* stage, we calculate Energy scores with and without the combination of MD, called EN and ENMD, respectively. We then used three post-rectification OOD detectors to predict task-id, BUILD: (i) ReAct, (ii) DICE, and (iii) SCALE using EN and ENMD scores. For a fair comparison, we analyze the results of BUILD with SM and SMMD and MORE with these post-rectification detectors.

4.2. Evaluation Protocol

We evaluate the (i) Closed-World performance, namely the classification of seen samples using ACA, AIA, and AF, and (ii) Open-World performance, namely the discriminative power on unseen samples using AUC and AUPR.

Closed-World Evaluation. For this evaluation, only test samples from the seen distribution are evaluated. At any given incremental step k , for any task $t \in \{1, 2, \dots, k\}$, all test samples belonging to tasks other than t are considered *near* OOD [35], i.e., $D_t = \bigcup_{i \neq t}^k D_i$, and the samples from t as In-Distribution (IND). We evaluate all classifier heads until the last trained head $\hat{f}_1, \dots, \hat{f}_k$ using the detectors mentioned in Sect. 2.2. The respective detectors produce an OOD score for each class, which is concatenated and compared to determine the task ID. We are basically choosing the class with the least OOD score or highest ID score, meaning the class with the highest probability of the sample belonging to that class’s distribution.

Open-World Evaluation. In this case, unlike before, test samples from both seen and unseen classes are evaluated. At any incremental step k , all test samples belonging to the seen distribution, i.e., D_1, \dots, D_k are considered ID, while any other classes outside the seen distribution: D_{k+1}, \dots, D_T , where T is the last class, are considered *far* OOD [35]. We measure the discriminative power of the OOD detector by evaluating AUC and AUPR on scores received from IND and OOD samples.

Evaluation metrics are computed for each incremental model until the last task. Closed-World metrics are computed from the second to the last task since there will not be any OOD data after the last task.

4.3. Results and Discussion

Here, we discuss the closed-world and open-world performance for each method: MORE-FW, MORE, BUILD as meta-rows for datasets: CIFAR10-5T, CIFAR100-10T, CIFAR100-20T as meta-columns in Table 1 and MORE-FW and BUILD for T-Imgnet200-5T and T-Imgnet200-10T in Table 2. Each meta-row is further categorized into the scoring function (or scorer) considered in this work: SM, SMMD, EN, and ENMD and then further into OOD detectors: Base, ReAct, DICE, and SCALE.

4.3.1. MORE: Baseline Performance

The reproduced results from the original work correspond to the SMMD scores and the Base detector in the table, which obtained better performances on the smallest dataset CIFAR10 and lower performances on the larger datasets. In a closed-world setting, considering LCA and AIA without AF and vice versa in isolation can be misleading. LCA and AIA suggest how well the model performs after learning new classes, AF shed light on how much the model forgets by the end since it first learns the task. For example, considering EN scores for all detectors LCA and AIA is higher for CIFAR10-5T compared to CIFAR100-10T and CIFAR100-20T but at the same time, AF is much higher for CIFAR10-5T, suggesting the model’s inability to perform correct task-id prediction on that dataset. Even if the model suffers in closed-world settings using EN scores, the detectors can still detect unseen samples, giving high AUC and AUPR performance. MORE performs best using SMMD scores.

4.3.2. MORE vs MORE-FW

After evaluating these models in closed- and open-world settings, we discovered that MORE-FW seems to perform better than the version proposed by the authors of that work (MORE) in many configuration settings, suggesting that additional training may, in fact, be unnecessary. We observed that, in SM and SMMD cases, MORE-FW gives a comparable or superior performance to MORE and does not suffer as much when using EN or ENMD scores. In fact, AF in this setting is the best across all methods. When using Base or SCALE as the OOD detector and SMMD or ENMD as the scoring function, we can achieve good performance in this setting.

4.3.3. BUILD Performance

While MORE and MORE-FW give good performance in certain settings, they both are trained using a buffer and, consequently, utilize more compute resources and take longer to train, as shown in Fig. 3. BUILD takes around one-third (half) of the memory usage and half the training time for CIFAR10 (CIFAR100) compared to MORE, and a similar memory usage but less than half of the training time compared to MORE-FW. On average, BUILD gives the best results and is stable across all the scoring functions. BUILD performs best using EN and ENMD scoring functions, giving the least AF for these settings. However, BUILD does not always supersede MORE and its variant in the setting of closed-world, especially when using the scoring functions SM and SMMD. When AF is the biggest concern, the best model is MORE-FW; however, it takes longer to train and it leverages the buffer, which, as we explained in the previous sections, creates privacy issues and may facilitate different adversarial attacks. BUILD performs consistently well on all detectors and scorers when compared to MORE and MORE-FW in the open-world setting and also in the closed-world setting when considering LCA and AIA. These results are substantiated by other dataset settings in Table 2.

Table 1: Results for MORE, MORE-FW, and BUILD on the CIFAR-10 and CIFAR-100 datasets, using different scorers and detectors, along with closed-world and open-world metrics.

		CIFAR10-5T					CIFAR100-10T					CIFAR100-20T					
		Closed-World			Open-World		Closed-World			Open-World		Closed-World			Open-World		
		LCA↑	AIA↑	AF↓	AUC↑	AUPR↑	LCA↑	AIA↑	AF↓	AUC↑	AUPR↑	LCA↑	AIA↑	AF↓	AUC↑	AUPR↑	
MORE-FW	SM	Base	88.51	92.23	2.54	90.71	95.93	64.45	74.16	2.04	79.71	93.88	64.44	75.00	2.56	78.98	96.22
		React	88.05	91.85	2.44	90.11	95.65	65.34	74.97	2.37	79.87	93.98	64.81	75.45	2.73	79.11	96.28
		Dice	86.28	91.10	3.72	89.17	95.34	52.50	65.74	1.08	76.99	92.78	59.28	71.13	2.59	76.40	95.52
		Scale	88.66	92.31	2.52	90.9	95.95	64.59	74.21	2.09	79.98	93.97	64.61	75.07	2.55	79.18	96.26
	SMMD	Base	86.06	91.16	1.79	85.16	93.01	71.73	80.47	3.13	80.65	94.36	70.15	79.98	4.54	78.15	96.32
		React	85.97	91.13	1.88	85.48	93.13	71.57	80.10	3.36	80.78	94.43	69.95	80.04	4.51	78.21	96.35
		Dice	86.97	91.78	2.10	86.66	93.78	58.79	70.38	1.27	79.68	94.20	67.14	77.55	3.33	78.57	96.41
		Scale	86.18	91.25	1.85	85.31	93.07	71.78	80.45	3.09	80.86	94.43	70.26	80.03	4.43	78.28	96.35
	EN	Base	77.53	87.68	14.96	85.24	93.44	38.26	55.26	27.93	72.08	91.47	25.11	41.12	27.05	67.20	93.73
		React	77.71	86.93	13.91	83.56	92.86	40.88	55.93	25.36	72.48	91.56	27.56	43.41	26.58	68.22	94.11
		Dice	79.92	89.38	7.66	82.50	92.30	5.83	27.64	40.50	62.03	86.31	8.35	25.39	29.40	61.19	91.65
		Scale	76.89	87.52	16.16	85.86	93.55	37.47	54.84	29.03	72.29	91.51	24.47	40.51	27.55	67.23	93.68
	ENMD	Base	90.15	94.02	2.06	90.16	95.85	69.05	78.25	10.30	80.36	94.37	65.91	75.80	10.08	78.78	96.56
		React	89.69	93.65	2.16	89.16	95.54	69.10	77.80	9.70	80.03	94.28	65.24	75.63	10.54	78.62	96.59
		Dice	88.55	93.27	1.99	88.46	95.11	53.98	66.62	22.59	74.15	92.00	56.86	69.03	15.93	75.18	95.76
		Scale	90.24	94.06	2.04	90.42	95.87	69.25	78.25	10.36	80.59	94.43	65.81	75.79	10.23	78.91	96.58
Avg.		85.46	91.21	4.99	87.43	94.40	56.54	68.44	12.14	77.03	93.00	54.37	66.31	11.54	75.14	95.52	
MORE	SM	Base	88.96	92.95	11.22	89.88	95.32	69.54	80.82	23.63	79.60	93.77	68.94	80.59	24.25	78.52	96.21
		ReAct	88.98	93.12	10.92	89.62	95.15	68.99	80.45	23.67	79.47	93.77	68.82	80.48	24.27	78.36	96.21
		DICE	85.92	91.36	14.78	88.90	94.97	55.48	72.90	38.17	72.61	91.61	61.55	75.86	32.47	74.03	95.32
		SCALE	88.93	92.93	11.22	89.86	95.24	69.53	80.84	23.67	79.70	93.82	68.98	80.60	24.23	78.57	96.23
	SMMD	Base	90.15	93.90	7.24	89.88	95.32	70.4	81.25	22.37	81.06	94.52	69.94	81.16	22.25	79.98	96.67
		ReAct	90.15	93.89	6.89	89.62	95.15	69.99	80.93	22.34	80.94	94.53	69.76	81.10	22.29	79.82	96.66
		DICE	89.03	93.28	9.21	88.90	94.97	57.38	73.98	36.12	74.70	92.76	62.53	76.70	31.23	76.16	96.13
		SCALE	90.16	93.92	7.27	89.86	95.24	70.36	81.25	22.40	81.15	94.57	69.94	81.18	22.29	80.03	96.68
	EN	Base	42.98	64.67	60.79	80.21	91.10	4.70	30.93	25.07	65.83	88.97	1.59	18.08	25.18	61.40	92.37
		ReAct	44.68	64.61	57.69	79.17	90.70	5.75	31.69	25.22	65.87	88.99	1.98	19.28	26.28	61.79	92.64
		DICE	46.93	69.71	55.41	81.14	91.46	1.87	17.68	11.99	59.71	85.23	0.41	12.00	15.41	58.18	90.89
		SCALE	42.44	64.36	61.66	80.84	91.25	4.53	30.88	25.26	66.16	89.12	1.48	17.90	24.98	61.59	92.37
	ENMD	Base	84.72	90.45	14.23	89.83	95.43	51.35	67.36	11.13	76.64	93.40	44.45	61.02	23.29	74.51	96.00
		ReAct	84.78	90.29	13.94	89.48	95.37	51.90	67.32	10.56	76.57	93.40	45.23	61.44	22.27	74.53	96.04
		DICE	83.90	90.09	14.86	88.88	94.78	37.99	54.67	-1.08	69.11	90.20	34.67	52.47	18.56	69.42	94.78
		SCALE	84.75	90.48	14.20	89.89	95.35	51.26	67.43	11.43	76.89	93.48	44.08	60.77	23.57	74.63	96.01
Avg.		76.72	85.63	23.22	87.25	94.18	46.31	62.52	20.75	74.13	92.01	44.65	58.79	23.93	72.60	95.08	
BUILD	SM	Base	86.63	91.27	6.36	92.09	96.36	62.90	74.17	13.36	79.29	93.54	59.41	71.96	14.23	78.21	96.17
		ReAct	86.63	91.27	5.79	91.56	96.04	63.68	74.81	12.69	79.32	93.57	59.77	72.42	14.23	78.11	96.16
		DICE	84.99	90.35	7.06	91.42	95.96	56.98	70.46	15.04	77.11	92.47	52.83	66.51	15.24	75.66	95.48
		SCALE	87.23	91.61	6.44	92.16	96.31	62.96	74.30	13.53	79.60	93.65	59.29	71.95	14.59	78.39	96.22
	SMMD	Base	84.64	90.01	3.04	84.49	92.65	71.48	80.44	8.99	79.51	94.04	66.86	77.28	9.42	75.06	95.76
		ReAct	84.56	89.99	3.18	84.71	92.74	71.65	80.39	8.78	79.85	94.18	67.26	77.55	9.53	75.42	95.83
		DICE	85.38	90.53	3.58	86.29	93.53	68.10	78.19	9.82	80.14	94.23	67.02	77.13	9.4	76.06	95.95
		SCALE	84.69	90.05	3.01	84.62	92.71	71.63	80.54	9.02	79.73	94.11	66.93	77.35	9.48	75.18	95.78
	EN	Base	88.06	92.59	6.52	87.93	94.24	69.41	79.48	10.79	79.39	93.53	62.90	75.26	13.87	75.32	95.52
		ReAct	86.94	91.92	5.80	87.28	94.06	68.64	78.79	10.63	79.38	93.55	63.13	75.51	13.54	75.89	95.65
		DICE	85.57	91.17	7.90	85.61	92.95	58.77	71.72	14.68	71.96	90.19	55.44	69.42	14.82	70.40	94.10
		SCALE	87.89	92.47	6.55	87.98	94.07	69.29	79.40	11.28	79.60	93.58	62.88	75.32	14.37	75.46	95.54
	ENMD	Base	89.81	93.66	3.65	90.35	95.63	73.47	82.16	8.61	81.02	94.48	68.98	79.11	10.37	78.35	96.43
		ReAct	88.75	92.97	3.42	89.71	95.43	72.91	81.64	8.48	80.70	94.40	68.47	78.95	10.58	78.21	96.42
		DICE	88.55	92.72	3.90	88.94	94.81	68.68	78.50	10.09	77.46	93.01	66.11	76.98	10.02	76.03	95.85
		SCALE	89.86	93.7	3.65	90.40	95.53	73.37	82.09	8.82	81.28	94.57	68.97	79.11	10.61	78.56	96.48
Avg.		86.89	91.64	4.99	88.47	94.56	67.75	77.94	10.91	79.08	93.57	63.52	75.11	12.14	76.27	95.83	

4.3.4. Rejection Performance

From the tables, we see that OOD methods are great at adding separability of IND from OOD samples, even in the absence of buffer data training. However, the main goal of detecting the unseen sample is to prevent the model from performing a classification and instead reject the sample. Fig. 2 showcases accuracy vs rejection curves i.e., how the accuracy of the mod-

els is affected at different rejection thresholds for CIFAR100-10T. Each row is the incrementally trained model, with a ratio of IND:OOD differing with each row, i.e., first row i.e., m_3 is a set of models after the model is trained on task t_3 (seen 40 classes and unseen 60 classes), therefore the ratio of IND:OOD is 40:60, for second row i.e., m_7 , is a set of models after training task t_7 . By that point, the model has been trained on 7 classes,

Table 2: Results for MORE-FW, and BUILD on the Tiny-Imagenet dataset, using different scorers and detectors, along with closed-world and open-world metrics.

		T-Imgnet200-5T					T-Imgnet200-10T					
		Closed-World			Open-World		Closed-World			Open-World		
		LCA↑	AIA↑	AF↓	AUC↑	AUPR↑	LCA↑	AIA↑	AF↓	AUC↑	AUPR↑	
MORE-FW	SM	Base	59.87	69.48	5.17	76.81	88.92	56.48	65.31	4.01	77.16	93.21
		ReAct	59.76	69.30	5.52	77.45	89.25	57.03	65.68	4.02	77.30	93.33
		DICE	53.03	63.04	4.02	75.45	87.82	49.68	59.76	3.07	75.60	92.56
		SCALE	59.97	69.57	5.23	76.96	88.98	56.52	65.27	3.96	77.27	93.22
	SMMD	Base	63.43	71.51	6.04	81.21	91.29	61.90	69.92	4.97	81.31	94.88
		ReAct	63.55	71.47	6.05	81.37	91.40	61.94	69.61	4.90	81.20	94.88
		Dice	57.46	65.81	4.21	80.68	91.24	55.26	64.41	3.52	81.12	94.94
		SCALE	63.43	71.50	6.14	81.31	91.34	61.97	69.94	4.91	81.43	94.91
	EN	Base	44.20	58.50	29.73	84.53	93.31	37.30	49.95	30.36	78.89	94.11
		ReAct	45.62	59.57	27.08	84.27	93.16	39.27	52.29	28.48	78.30	93.93
		DICE	27.37	46.04	40.46	79.49	90.65	17.25	33.82	40.63	73.30	92.26
		SCALE	43.66	58.26	30.52	84.70	93.38	37.06	49.92	30.66	79.11	94.21
	ENMD	Base	60.60	69.30	13.56	86.65	94.33	59.97	67.41	12.33	84.17	96.18
		ReAct	61.07	69.51	12.26	86.32	94.16	59.95	67.77	12.11	83.73	96.06
		DICE	46.83	58.98	23.59	84.21	93.15	46.16	56.86	21.16	81.09	95.32
		SCALE	60.36	69.26	13.80	86.90	94.43	59.65	67.24	12.44	84.47	96.25
	Avg.		54.39	65.07	14.59	81.77	91.68	51.09	60.95	13.85	79.72	94.39
BUILD	SM	Base	56.85	66.93	11.69	77.50	89.05	52.36	62.57	11.39	76.58	93.14
		React	56.96	66.97	11.50	77.85	89.28	52.73	62.86	11.14	76.99	93.35
		Dice	51.97	62.39	11.76	76.30	88.07	48.47	59.14	11.99	75.45	92.68
		Scale	56.84	66.97	11.83	77.64	89.11	52.43	62.63	11.42	76.73	93.18
	SMMD	Base	62.23	70.18	10.18	81.59	91.36	60.97	68.95	9.44	80.94	94.77
		React	62.06	70.24	10.18	81.69	91.45	60.46	68.33	9.30	81.01	94.82
		Dice	57.85	66.24	9.86	81.08	91.10	57.21	65.12	9.39	81.00	94.84
		Scale	62.14	70.19	10.29	81.65	91.39	60.90	68.89	9.53	81.04	94.79
	EN	Base	64.64	71.98	8.21	85.96	93.70	61.73	69.88	10.18	84.47	96.05
		React	64.38	71.65	7.93	85.64	93.55	61.25	69.17	9.77	83.91	95.90
		Dice	56.90	65.66	11.25	83.18	92.25	54.80	64.10	12.01	81.88	95.24
		Scale	64.67	71.96	8.26	86.00	93.68	61.82	70.02	10.28	84.60	96.06
	ENMD	Base	66.34	72.84	7.98	87.29	94.38	64.56	71.82	9.19	85.76	96.53
		React	66.23	72.66	7.56	86.99	94.24	63.93	71.13	8.99	85.27	96.39
		Dice	60.60	67.95	10.00	86.19	93.81	59.49	66.98	9.90	84.73	96.21
		Scale	66.30	72.80	8.00	87.42	94.43	64.60	71.79	9.09	85.95	96.58
	Avg.		61.06	69.23	9.78	82.75	91.93	58.61	67.09	10.19	81.64	95.03

making the ratio 80:20 and so on until m_8 , where the model will have seen 90% of the classes and rejection is performed only on 10% of the data. Each column represents each detector. The individual plot compares the performance of the three methods: MORE-FW, MORE, and BUILD when using the scoring function with which they perform better (SMMD for MORE and MORE-FW and ENMD for BUILD). Their performances are comparable.

4.3.5. Scoring Functions

We observe that Softmax-based scores, i.e., SM and SMMD are the best performing scorers for MORE-FW and MORE methods, whereas Energy-based scorers i.e., EN and ENMD for BUILD. We also note that using Mahalanobis Distance with SM and EN almost always helps improve performance in both closed- and open-world settings, especially by greatly reducing AF.

4.3.6. OOD Detectors

Generally speaking, all detectors obtain very close performances for all evaluation metrics across datasets. Base and SCALE are the overall best detectors in all methods and scorers.

4.3.7. Train Time Performance

Memory buffers contribute a lot to the large memory consumption of the models. For example, raw images from CIFAR datasets of size $32 \times 32 \times 3$ in a buffer of size 2000 are approximately 6.1M vector values, similarly for TinyImageNet200, it's 24.6M ($64 \times 64 \times 3$) vector values. Processing 6.1M or 24.6M elements in each incremental training step for MORE-FW and additionally again during backupupdate step in MORE leads to almost double the Maximum Memory Usage (MMU) for MORE-FW and more than triple for MORE compared to BUILD that, has no buffer (see Fig. 3). We also observed that buffered methods take longer to achieve the desired training accuracy than their buffer-free counterparts. For example, when training CIFAR100-10T in Fig. 4, BUILD reaches the 90% training accuracy at the fifth epoch, whereas it takes around 40 epochs for MORE-FW to achieve similar performance.

5. Related Work

Although there is a wealth of work in CL and OOD domains individually, there are few works that adopted TIL methods to perform CIL with task-id prediction in an open-world setting.

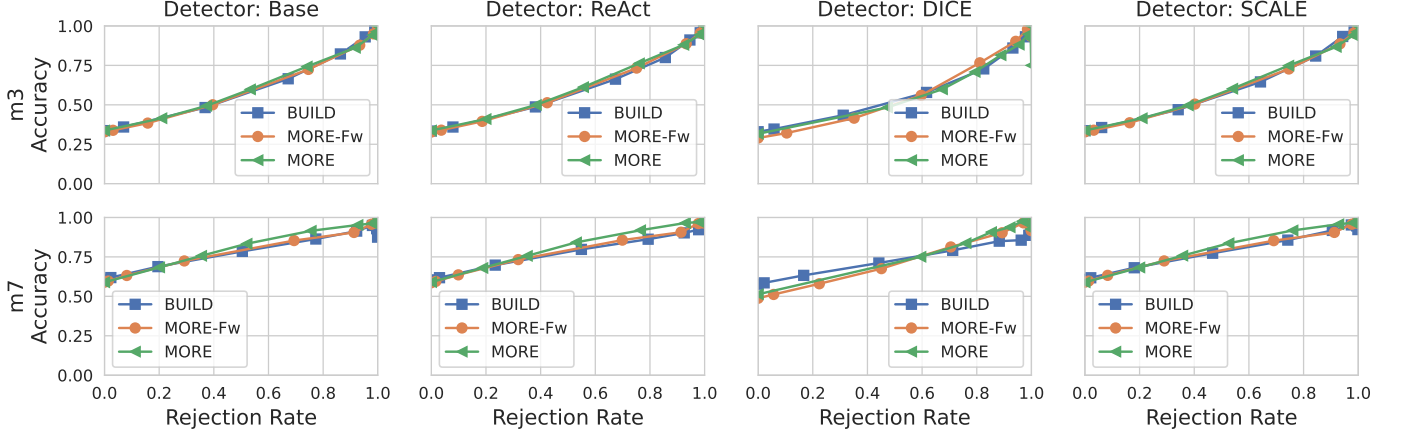


Figure 2: Accuracy vs Rejection Curve for Cifar100-10T: Here we plot the models with their corresponding best scoring functions for all detectors (columns): SMMD for MORE and MORE-Fw and ENMD for BUILD. Each row is the intermediate model. For each plot, x-axis is the rejection rate and y-axis is the accuracy of the intermediate model

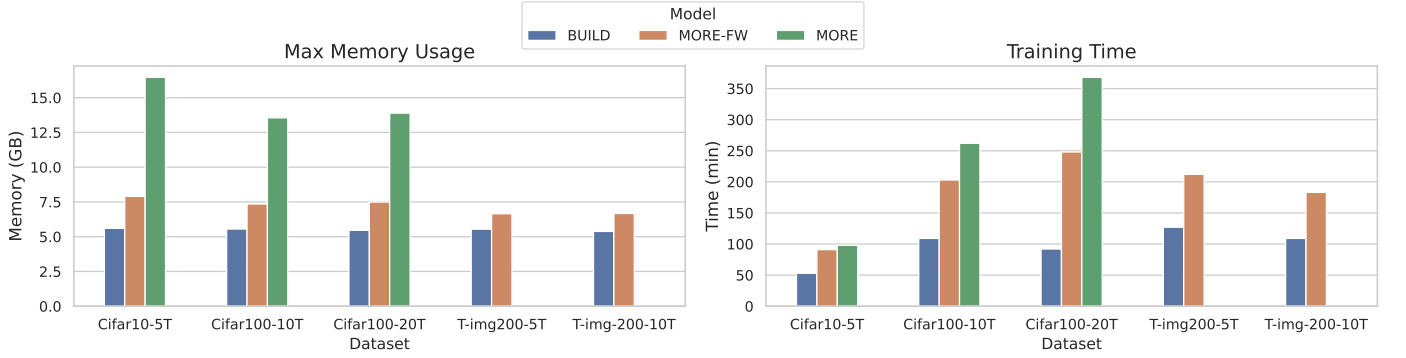


Figure 3: (a) Max Memory Usage and (b) Total training time, evaluated for each model and dataset

MORE [15] uses OOD detection for task-id prediction, replays the sample at first, in the forward train, and then backupdates the heads. ROW [16], is empirically similar to MORE, with added theoretical proofs of learnability of CIL. TPL [17] is trained as MORE but uses the likelihood ratio as the OOD detection score. CEDL [36], integrates deep evidential learning [37] into CL approaches that use an incremental buffer. However, all these works use buffers in their pipeline to replay at the time of training. Even though they considered open-world setting, they do not elaborate their evaluation to rejection performance, which is the goal of OOD detection in the first place.

Then, a few works in the OOD literature attempt to incorporate IL into their pipeline. OOD-UCL [38] performs OOD detection by correcting output bias on unsupervised CL. OSIL [39] performs novel class detection using clustering and appends the new classes to known classes to train natural language data. KNNENS [40] performs novel class detection using k -nearest neighbor and then storing them to a buffer to be incorporated into training. Most works in the OOD domain that uses IL in their pipeline consider IL as a subsequent step after detecting and storing novel classes in memory. None of these works align with the IL assumption of unavailability of old samples and adopting measures to prevent forgetting. In this work, we

detect OOD samples while learning new classes. BUILD performs OOD detection and evaluates the accuracy of the model based on the rejection ratio of the detected samples, giving a realistic view of model deployment in the wild.

6. Conclusion, Limitations and Future Work

Class-incremental learning in the real world must also be performed in an open-world setting. In this work, we have first considered MORE, one of the best performing IL approaches that consider an open-world setting. We have performed an extensive experimental analysis where we have considered more scoring functions and detectors with respect to those employed in MORE. Then, we have compared these systems with BUILD, a method proposed in this work that does not employ a replay buffer or requires the need of backupdating the weights. The experimental analysis shows that it can be trained in less than half the time while providing comparable performances with MORE. When compared with MORE-Fw, a buffer-less variant of MORE, it can be trained in half the time and provides comparable performance considering all metrics except the average forgetting, which is higher for BUILD. We also extended our analysis to evaluate accuracy at varying rejection rate of

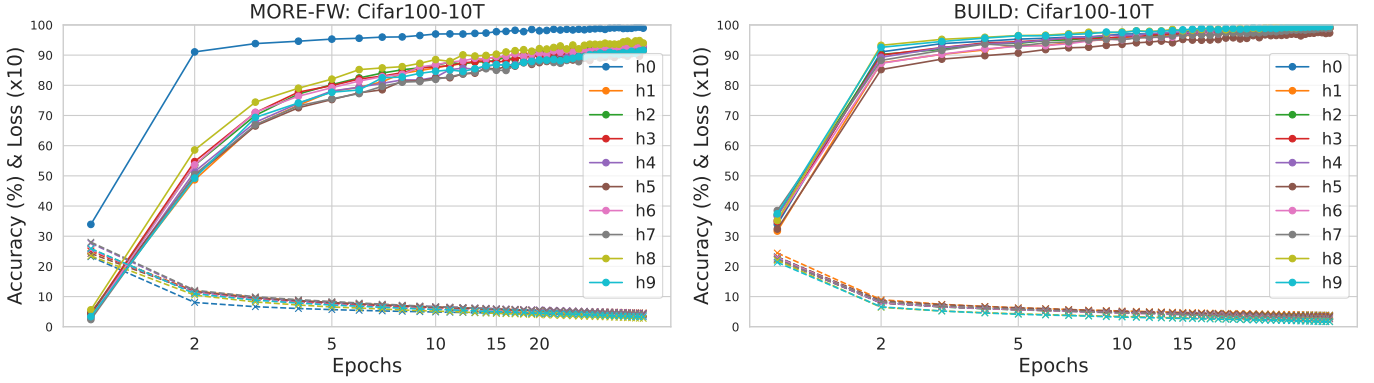


Figure 4: Training accuracy and loss for CIFAR100-10T for MORE-Fw and BUILD. Note here, the left plot is after the forward pass, to get the final training, backupdates does additional training.

the competing models, revealing that BUILD gives competitive performance when compared with other methods, while being highly stable on various scoring functions, unlike MORE and variants that suffers performance when using Energy scores. Our proposed method, being bufferless, resolves the privacy concern and the higher vulnerability caused by the presence of a buffer with a slight trade-off with average forgetting. We believe that the higher average forgetting is a limitation of the proposed approach that can be addressed in future work.

Acknowledgments

This work has been partly supported by the EU-funded Horizon Europe projects ELSA (GA no. 101070617), Sec4AI4Sec (GA no. 101120393) and CoEvolution (GA no. 101168560); and by the projects SERICS (PE00000014) and FAIR (PE00000013) under the MUR National Recovery and Resilience Plan funded by the European Union - NextGenerationEU. This work was conducted while Srishti Gupta was enrolled in the Italian National Doctorate on AI run by Sapienza University of Rome in collaboration with the University of Cagliari.

References

- [1] M. Poyer, T. P. Breckon, Neural architecture search: A contemporary literature review for computer vision applications, *Pattern Recognition* 147 (2024) 110052. doi:<https://doi.org/10.1016/j.patcog.2023.110052>.
- [2] T. B. Brown, B. Mann, N. Ryder, M. Subbiah, J. Kaplan, P. Dhariwal, A. Neelakantan, P. Shyam, G. Sastry, A. Askell, S. Agarwal, A. Herbert-Voss, G. Krueger, T. Henighan, R. Child, A. Ramesh, D. M. Ziegler, J. Wu, C. Winter, C. Hesse, M. Chen, E. Sigler, M. Litwin, S. Gray, B. Chess, J. Clark, C. Berner, S. McCandlish, A. Radford, I. Sutskever, D. Amodei, Language models are few-shot learners, in: *Annual Conf. on Neural Information Processing Systems*, 2020.
- [3] W. J. Scheirer, A. de Rezende Rocha, A. Sapkota, T. E. Boulton, Toward open set recognition, *IEEE Trans. Pattern Anal. Mach. Intell.* 35 (7) (2013) 1757–1772.
- [4] F. Condessa, J. Bioucas-Dias, J. Kovačević, Performance measures for classification systems with rejection, *Pattern Recognition* 63 (2017) 437–450. doi:<https://doi.org/10.1016/j.patcog.2016.10.011>.
- [5] E. Strubell, A. Ganesh, A. McCallum, Energy and policy considerations for deep learning in NLP, in: *Proceedings of the 57th Annual Meeting of the Association for Computational Linguistics*, 2019, pp. 3645–3650. doi:10.18653/v1/P19-1355.
- [6] D. Hendrycks, K. Gimpel, A baseline for detecting misclassified and out-of-distribution examples in neural networks, in: *Int. Conf. on Learning Representations*, 2017.
- [7] W. Liu, X. Wang, J. D. Owens, Y. Li, Energy-based out-of-distribution detection, in: *Annual Conf. on Neural Information Processing Systems* 2020, 2020.
- [8] L. Wang, X. Zhang, H. Su, J. Zhu, A comprehensive survey of continual learning: Theory, method and application, *IEEE Trans. on Pattern Analysis and Mach. Intel.* 46 (8) (2024) 5362–5383. doi:10.1109/TPAMI.2024.3367329.
- [9] C. Liu, Y. Wang, D. Li, X. Wang, Domain-incremental learning without forgetting based on random vector functional link networks, *Pattern Recognition* 151 (2024) 110430. doi:<https://doi.org/10.1016/j.patcog.2024.110430>.
- [10] M. De Lange, R. Aljundi, M. Masana, S. Parisot, X. Jia, A. Leonardis, G. Slabaugh, T. Tuytelaars, A continual learning survey: Defying forgetting in classification tasks, *IEEE Trans. on pattern analysis and mach. Intel.* 44 (7) (2021) 3366–3385.
- [11] J. Serrà, D. Suris, M. Miron, A. Karatzoglou, Overcoming catastrophic forgetting with hard attention to the task, in: *Int. Conf. on Mach. Learning*, Vol. 80, 2018, pp. 4555–4564.
- [12] G. M. van de Ven, A. S. Tolias, Three scenarios for continual learning (2019).
- [13] M. Masana, X. Liu, B. Twardowski, M. Menta, A. D. Bagdanov, J. Van De Weijer, Class-incremental learning: survey and performance evaluation on image classification, *IEEE Trans. on Pattern Analysis and Mach. Intel.* 45 (5) (2022) 5513–5533.
- [14] G. Kim, C. Xiao, T. Konishi, Z. Ke, B. Liu, A theoretical study on solving continual learning, in: *Annual Conf. on Neural Information Processing Systems* 2022, 2022.
- [15] G. Kim, B. Liu, Z. Ke, A multi-head model for continual learning via out-of-distribution replay, in: *Conf. on Lifelong Learning Agents*, PMLR, 2022, pp. 548–563.
- [16] G. Kim, C. Xiao, T. Konishi, B. Liu, Learnability and algorithm for continual learning, in: *Int. Conf. on Mach. Learning*, Vol. 202, 2023, pp. 16877–16896.
- [17] H. Lin, Y. Shao, W. Qian, N. Pan, Y. Guo, B. Liu, Class incremental learning via likelihood ratio based task prediction, in: *Int. Conf. on Learning Representations*, 2024.
- [18] A. E. Cinà, K. Grosse, A. Demontis, S. Vascon, W. Zellinger, B. A. Moser, A. Oprea, B. Biggio, M. Pelillo, F. Roli, Wild Patterns Reloaded: A Survey of Machine Learning Security against Training Data Poisoning, *ACM Computing Surveys* 55 (13s) (2023) 294:1–294:39. doi:10.1145/3585385.
- [19] M. Rigaki, S. Garcia, A Survey of Privacy Attacks in Machine Learning, *ACM Comput. Surv.* 56 (4), place: New York, NY, USA Publisher: Association for Computing Machinery (2023). doi:10.1145/3624010.
- [20] D.-W. Zhou, Q.-W. Wang, Z.-H. Qi, H.-J. Ye, D.-C. Zhan, Z. Liu, Class-incremental learning: A survey, *IEEE Transactions on Pattern Analysis and Machine Intel.* 46 (12) (2024) 9851–9873. doi:10.1109/TPAMI.2024.3429383.

- [21] K. Lee, K. Lee, H. Lee, J. Shin, A simple unified framework for detecting out-of-distribution samples and adversarial attacks, in: Annual Conf. on Neural Information Processing Systems, pages = 7167–7177, 2018.
- [22] Y. Sun, C. Guo, Y. Li, React: Out-of-distribution detection with rectified activations, in: Annual Conf. on Neural Information Processing Systems 2021, 2021, pp. 144–157.
- [23] Y. Sun, Y. Li, DICE: leveraging sparsification for out-of-distribution detection, in: ECCV (24), Vol. 13684 of Lecture Notes in Computer Science, 2022, pp. 691–708.
- [24] K. Xu, R. Chen, G. Franchi, A. Yao, Scaling for training time and post-hoc out-of-distribution detection enhancement, in: Int. Conf. on Learning Representations, 2024.
- [25] S. Rebuffi, A. Kolesnikov, G. Sperl, C. H. Lampert, icarl: Incremental classifier and representation learning, in: 2017 IEEE Conf. on Computer Vision and Pattern Recognition, 2017, pp. 5533–5542. doi:10.1109/CVPR.2017.587.
- [26] N. Houlsby, A. Giurghi, S. Jastrzebski, B. Morrone, Q. de Laroussilhe, A. Gesmundo, M. Attariyan, S. Gelly, Parameter-efficient transfer learning for NLP, in: Int. Conf. on Mach. Learning, Vol. 97, 2019, pp. 2790–2799.
- [27] Z. Ke, B. Liu, X. Huang, Continual learning of a mixed sequence of similar and dissimilar tasks, in: Annual Conf. on Neural Information Processing Systems 2020, 2020.
- [28] A. Mallya, S. Lazebnik, Packnet: Adding multiple tasks to a single network by iterative pruning, in: 2018 IEEE Conf. on Computer Vision and Pattern Recognition, 2018, pp. 7765–7773. doi:10.1109/CVPR.2018.00810.
- [29] M. Wortsman, V. Ramanujan, R. Liu, A. Kembhavi, M. Rastegari, J. Yosinski, A. Farhadi, Supermasks in superposition, in: Annual Conf. on Neural Information Processing Systems 2020, 2020.
- [30] Wild patterns: Ten years after the rise of adversarial machine learning 84. doi:10.1016/j.patcog.2018.07.023.
- [31] S. Lu, Y. Wang, L. Sheng, A. Zheng, L. He, J. Liang, Recent advances in ood detection: Problems and approaches (2024).
- [32] H. Touvron, M. Cord, M. Douze, F. Massa, A. Sablayrolles, H. Jégou, Training data-efficient image transformers & distillation through attention, in: Int. Conf. on Mach. Learning, Vol. 139, 2021, pp. 10347–10357.
- [33] A. P. Bradley, The use of the area under the roc curve in the evaluation of machine learning algorithms, Pattern Recognition 30 (7) (1997) 1145–1159. doi:https://doi.org/10.1016/S0031-3203(96)00142-2.
- [34] T. Saito, M. Rehmsmeier, The precision-recall plot is more informative than the roc plot when evaluating binary classifiers on imbalanced datasets, PloS one 10 (3) (2015) e0118432.
- [35] J. Zhang, J. Yang, P. Wang, H. Wang, Y. Lin, H. Zhang, Y. Sun, X. Du, Y. Li, Z. Liu, et al., Openood v1. 5: Enhanced benchmark for out-of-distribution detection, ArXiv preprint abs/2306.09301 (2023).
- [36] E. Aguilar, B. Raducanu, P. Radeva, J. V. de Weijer, Continual evidential deep learning for out-of-distribution detection (2023). arXiv: 2309.02995.
- [37] M. Sensoy, L. M. Kaplan, M. Kandemir, Evidential deep learning to quantify classification uncertainty, in: Annual Conf. on Neural Information Processing Systems, 2018, pp. 3183–3193.
- [38] J. He, F. Zhu, Out-of-distribution detection in unsupervised continual learning, in: IEEE/CVF Conf. on Computer Vision and Pattern Recognition WS, 2022, pp. 3849–3854. doi:10.1109/CVPRW56347.2022.00430.
- [39] J. Leo, J. Kalita, Moving towards open set incremental learning: Readily discovering new authors (2019).
- [40] J. Zhang, T. Wang, W. W. Y. Ng, W. Pedrycz, Knnens: A k-nearest neighbor ensemble-based method for incremental learning under data stream with emerging new classes, IEEE Trans. on Neural Net. and Learning Systems 34 (11) (2023) 9520–9527. doi:10.1109/TNNLS.2022.3149991.